Homological Region Adjacency Tree for a 3D Binary Digital Image via HSF Model

Pedro Real[1], Helena Molina-Abril[1], Fernando Díaz-del-Río[1], and Sergio Blanco-Trejo[2]

[1] H.T.S. Informatics' Engineering, University of Seville, Seville, Spain
{real,habril,fdiaz}@us.es
[2] Department of Aerospace Engineering and Fluid Mechanics, University of Seville, Seville, Spain
sblanco1@us.es

Abstract. Given a 3D binary digital image I, we define and compute an edge-weighted tree, called *Homological Region Tree* (or Hom-Tree, for short). It coincides, as unweighted graph, with the classical Region Adjacency Tree of black 6-connected components (CCs) and white 26-connected components of I. In addition, we define the weight of an edge (R, S) as the number of tunnels that the CCs R and S "share". The Hom-Tree structure is still an isotopic invariant of I. Thus, it provides information about how the different homology groups interact between them, while preserving the duality of black and white CCs.

An experimentation with a set of synthetic images showing different shapes and different complexity of connected component nesting is performed for numerically validating the method.

Keywords: Binary 3D digital image · Region Adjacency Tree · Combinatorial topology · Homological Spanning Forest

1 Introduction

A classic scheme in most image understanding algorithms always includes two important initial steps: (a) [segmentation] partition into regions and (b) [region connectivity representation] data structure specifying the connectivity relationships between the regions of this segmentation.

The vast majority of the region connectivity representations used are based on the mathematical concept of graph. The most notorious example of this kind of representation is the region adjacency graph (RAG, for short) [23]. The reasoning used in RAG is based on two topological properties: adjacency and inclusion. In the case of 3D digital images, the most usual adjacency relationships

Work supported by the Spanish research projects TOP4COG:MTM2016-81030-P (AEI/FEDER, UE), COFNET (AEI/FEDER, UE) and the VPPI of University of Seville.

between cubical voxels employed to be extended in determining edges of the region adjacency graph are 6, 18 and 26-adjacencies. Two cubical voxels are 6, 18 or 26-adjacent if they share a common face, edge, or vertex. To prevent topological paradoxes and, at the same time, to benefit from strong topological duality properties, we specify 6-adjacency between black voxels and 26-adjacency between white voxels or, in other words, we use a $(6, 26)$-image.

In order to exclusively highlight the ambient isotopic property "to be surrounded by" (inclusion) as an adjacency relationship between regions or boundaries of regions, the notion of *Region-Adjacency Tree* (or RAG tree, for short) (also called *homotopy tree*, *inclusion tree* or *topological tree*) was created [23,24]. Restricted to binary 2D digital images, the RAG tree contains all the homotopy type information of the foreground (FG) (black object according to our convention) but the converse is, in general, not true [24]. Aside from image understanding applications [5], RAG trees have encountered exploitation niches in geoinformatics, computer aided design, rendering, dermatoscopics image, biometrics,... [1,4–6].

Focusing on homotopy-based representation models of digital objects and images, there are numerous works that arise from sources of digital topology (for instance, [14]), continuous or cellular topology [16] and nD shape search [3] with three clearly differentiated notions: Reeb graphs [7], skeletons [2,12] and boundary representations [17].

Given a binary 3D digital image I, an edge-weighted graph structure, called *Homological Region Tree* (Hom-Tree, for short), which, as unweighted graph, coincides with the classical Region Adjacency Tree of black 6-connected components and white 26-connected components of I I. The weight of an edge (R, S) is the number of tunnels that the CCs R and S of opposite color "share" (that is, those whose have a same root node).

The unique Hom-Tree representation is computed here from a complete and flexible homotopy model for I (considered as a cubical complex) called Homological Spanning Forest (or HSF, for short) [9,18,19]. Seen as segmentations, the Hom-Tree can be obtained from the topological "over-segmentation" HSF, via a suitable region merging. The elementary merging operation involves two cells of dimensions differing in one and can be redefined as homotopy operations on the cell complex analogous of I [15].

The contribution of this paper relies on the definition of the compact Hom-tree data structure and of its topological properties. In particular, following [13], two nD pictures are topologically equivalent iff their rooted RAG trees are isomorphic, where the background (BG) defines the root for both pictures. Within the context of 3D binary digital images, Hom-Tree appears to be one tool allowing to coherently define a new refined notion of nD topological equivalence.

The paper has the following sections. Section 2 is devoted to recall the machinery for computing the structures needed for HSF construction. Next, an algorithm for constructing a Hom-Tree from a HSF structure is showed in Sect. 3. Section 4 is devoted to an experimentation with a set of synthetic images showing

different shapes and different complexity of connected component nesting for numerically validating the method. Finally, the conclusions are summarized.

2 HSF Structure Seen as an Over-Segmentation

In this section, we recall the constituting parts of a HSF representation of I and stress its close relationship with the Euler numbers of the CCs of I. For technical details of the algorithm for constructing a HSF structure, see [9,21].

From now on, when we refer to a digital image I or digital object $S \subset I$, it can be indistinctly understood as a spatial matrix linked to a cubical grid or as a finite abstract cubical complex (homotopically equivalent to the semi-continuous analog of I or S). Let us recall that an abstract cell complex (ACC) is a particular locally finite space in which a dimension is defined for each cell and each k-cell (cell of dimension k, $k \geq 1$) has a boundary set $Bd(c)$ of $(k-1)$-cells and a coboundary set $Cb(c)$ of $(k+1)$-cells. Usually, as is our case here, the coboundary set of the cells is completely determined by their boundary set (or viceversa). The cells of I live in its auto-dual cubical grid and they can be voxels, pair of voxels, 4-uples of voxels and 8-uples of voxels.

The goal of a topological graph-based data structure of a binary nD digital image is to save cells (given at inter-n-xel level) and incidence relationships between them, in such a way that, for correctly and efficiently retrieving global topological information of I (for example, connected components, region's Euler number,...), only graph transformations over the structure are needed. HSF data structures completely meet this objective. Roughly speaking, a HSF structure on a $(6, 26)$-image is a graded set of graphs of cell-nodes, that appropriately extend to higher dimension the classical algorithm of labeling connected components of a digital image via a spanning forest covering all the voxels [20].

Given an binary image I with set of black 6-CCs $\{R_1, \ldots, R_m\}$ and set of white 26-CCs $\{S_1, \ldots, S_n\}$, the output of the HSF construction algorithm provides us for each black or white CC R, a set of graphs that, in a particular maximal and non-redundant way, cover all the cells of R at inter-voxel level. Each graph of this kind has as nodes k-cells and $(k+1)$-cells ($k \geq 0$) and it is denoted as $(k, k+1)$-graph. A $(k, k+1)$-graph G is essential (resp. inessential) if $\chi(G) = \sharp\{k\text{-cell nodes of } G\} \setminus \sharp\{(k+1)\text{-cell nodes of } G\}$ (where $\sharp$ means cardinality of a set) is different from zero (resp. zero). Anyway, for each CC R of I, there is exactly one essential $(0, 1)$-tree and the Euler number $\chi(R)$ of R as cell complex (that is, $\chi(R) = \sharp\{0\text{-cells in } R\} - \sharp\{1\text{-cells in } R\} + \sharp\{0\text{-cells in } R\}$) agrees with the alternate sum

$$1 \; - \sum_{G \in (1,2)\text{-graph of } R} \chi(G) \; + \sum_{G \in (2,3)\text{-graph of } R} \chi(G).$$

Let us note that $\sum_{G \in (0,1)\text{-graph of } R} \chi(G) = 1$. Moreover, $\chi(R)$ can also be expressed in global topological terms as $\chi(R) = \sharp\{\text{CC of } R\} - \sharp\{\text{tunnels of } R\} + \sharp\{\text{cavities of } R\} = 2 - \sharp\{\text{tunnels of } R\}$.

For representing the homological characteristics of the CCs of I in terms of simple cells, we need to place vectors (c, c') (c being a k-cell and c' being a neighbor $(k+1)$-cell) on the HSF-graphs in a maximal way and satisfying that any cell is in one vector at most (see [10]). Hence, only in the essential HSF $(k, k+1)$-graphs, there are k-cells, called *critical cells*, that remain unpaired. Let us limit to say here that the combinatorial homology classes of any region R are intimately associated to the critical cells of its essential HSF-graphs and, in particular, the number of tunnels of R agrees with the number of its critical 1-cells.

This particular region-growing strategy at inter-voxel level is sequentially guided by two criteria: (a) [merging through boundary] A k-cell c (cell of dimension k ($k \geq 1$) and all the $(k-1)$-cells of $Bd(c)$ are included as nodes in an essential HSF-graph G of dimension $(k-1, k)$ (composed of $(k-1)$-cells and k-cells) if there is an odd number of cells of $Bd(c)$ belonging to G and (b) [region color similarity] We give to each cell a unique color and a color-dependant dimension. Then, region color similarity at inter-voxel level is prioritized. In the parallel version of the HSF construction algorithm of [21], the idea is different from the previous one and it is based in the cellular technique of crack transport [9].

3 Hom-Tree Seen as a Homological Segmentation

The underlying idea behind the RAG Tree of the binary 3D digital $(6, 26)$-image I is that I can be naturally segmented as a set of black 6-CCs $\{R_1, \ldots, R_m\}$ and a set of white 26-CCs $\{S_1, \ldots, S_n\}$, and any such region can have one or two 6-neighbor regions specified by the inclusion condition. In fact, given a 6-neighbor region of voxels R_i (for instance, a black 6-CC) and a S_j (a white 26-CC):

- R_i is surrounded by S_j or S_j is surrounded by R_i.
- its intersection $R_i \cap S_j$ is always a connected frontier cubical complex at inter-voxel level.
- As cubical complexes, if R_i is surrounded by S_j and S_j has a non-null number of tunnels, at least there is one tunnel of S_j that is shared with R_i.

Given a 3-tuple of regions, it is evident that its common intersection is always $\emptyset$. Taking into account that the topological Euler number of a segmented solid satisfy the inclusion-exclusion principle, we have in the contractile case of I:

$$1 = \sum_i \chi(R_i) \; + \; \sum_i \chi(S_i) \; - \; \sum_{i,j} \chi(R_i \cap S_j).$$

This last equality can be decomposed in terms of CCs, tunnels and cavities of the regions of $\{R_i\}$ and $\{S_j\}$ is as follows:

- In terms of CCs, we have:

$$\sum_{i,j} \sharp\{\text{CCs of } R_i \cap S_j\} = (m+n) - 1$$

– In terms of tunnels, we have:

$$\sum_i \sharp\{\text{tunnels of } R_i\} + \sum_i \sharp\{\text{tunnels of } S_i\} \;=\; \sum_{i,j} \sharp\{\text{tunnels of } R_i \cap S_j\}$$

– In terms of cavities, we have:

$$\sum_i \sharp\{\text{cavities of } R_i\} + \sum_i \sharp\{\text{cavities of } S_i\} \;=\; \sum_{i,j} \sharp\{\text{cavities of } R_i \cap S_j\}$$

In consequence,

$$\sum_i \sharp\{\text{tunnels of } R_i\} \;=\; \sum_i \sharp\{\text{tunnels of } S_i\}) \;=\; \frac{1}{2} \cdot \sum_{i,j} \sharp\{\text{tunnels of } R_i \cap S_j\}.$$

Then, taking advantage of the duality properties of the homological characteristics of the black 6-CCs and white 26-CCs, we can deduce a new isotopic invariant of I, by adding weights to the edges of the rooted classical RAG tree of I. This tree is called *Homological Region Tree* (or *Hom-Tree*, for short) and the weight of the edge (R, S) is given by the number of tunnels the CCs R and S share.

In order that an algorithm for computing a HSF structure of I could be correctly adapted to the computation of the Hom-Tree (see Fig. 1), we first need to work on the auto-dual cubical grid, specifying the contribution of each black and white set C of eight mutually 6-adjacent voxels to the global computation of an HSF for I and for its corresponding CCs. For instance, if we have a set C of this type with only one white voxel: (a) its contribution in terms of cells to a black 26-CC is of 1 0-cells, 6 1-cells, 11 2-cells and 7 3-cells; (b) its contribution in terms of cells to a white 6-CC is reduced to one 0-cell. In this way, each inter-voxel element of the auto-dual cubical grid is endowed with a unique color and with a color-dependent dimension, before constructing an HSF for I.

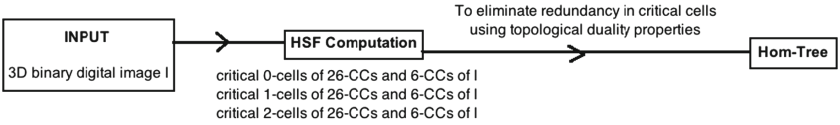

Fig. 1. Scheme of the Hom-Tree computation via HSF

Let us note that the cells of an inter-voxel frontier cubical complex between two regions R_i and S_j still belong to the auto-dual cubical grid. Let us note that it can be identified with a connected boundary surface (cubical complex) that is the intersection of the set of physical voxels of R_i with than that of S_j.

Finally, for obtaining the Hom-Tree from the set of critical 0, 1 and 2-cells of the different black 6-CCs and white 26-CCs of I, we need to apply boundary

and coboundary operations to the critical cells in order to: (a) to pair by duality black critical 0-cells (CCs) with white critical 2-cells (cavities) and vice-versa; and (b) to pair by duality critical 1-cells (tunnels) of a black 6-CC with critical 1-cells of a white neighbor 26-CC. After Step (a), the edges of the RAG Tree of I are determined. After Step (b), the weights of the edges are defined (Fig. 2).

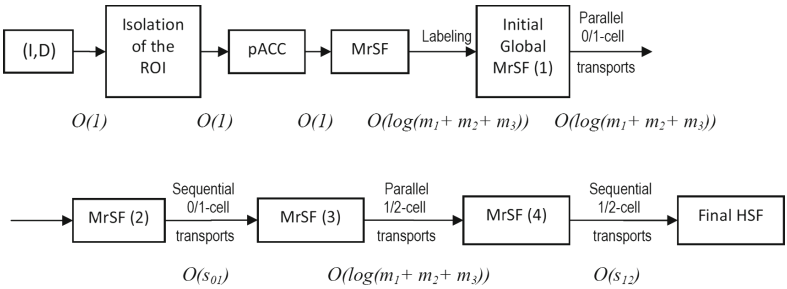

Fig. 2. Time orders for the different steps of HSF computation in [21], having $m_1 \times m_2 \times m_3$ computation processors. s_{01} and s_{12} are the number of sequential cancellations of remaining 0/1 and 1/2 cells respectively (after the parallel cancellation of these pairs).

4 Experimentation

Part of the experimentation of the new proposed method has been done using an automatic homotopy deformation (thinning-thickening) tool based on the notion of 3D simple point that has been developed for this purpose. For algorithmic details, see [2].

The idea is to corroborate with our HSF computation software that homotopically (in fact, isotopically) equivalent shape nestings return the same Hom-Tree.

Then, we use the thinning-thickening algorithm to randomly deform three synthetic image examples, and then use these modified shapes to validate the property of isotopy-invariance of the Hom-Tree. Up to 500 26-simple points have been randomly added/removed 100 times for each of these cases: Three concentric spheres, one torus with two spheres inside, and one sphere with two spheres inside (see Fig. 3).

In the rest of the section we present briefly the HSF tool that allows us to compute the Hom-tree of several binary 3D images. Previous version of our HSF software was presented in [9] for binary 2D images, and in [8] for color 2D images. Additionally, in [22] the scaffolding of tridimensional HSF and a unpretentious software was published. That preliminary version could not do support transports of cracks. We are now developing a complete HSF software with emphasis in its parallel computation of all of its stages.

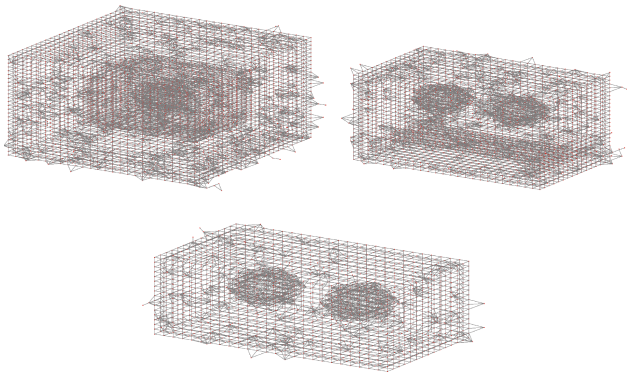

Fig. 3. Examples of deformed objects: Three concentric spheres, one torus with two spheres inside, and one sphere with two spheres inside.

In a nutshell, and as it is shown in Fig. 4, HSF software is based on an abstract cubical complex (ACC) of a 3D digital image. In this Figure, 0-cells, 1-cells, 2-cells and 3-cells are represented by circles, triangles, squares and stars respectively. At the left bottom of the figure there is a representation of a voxel as a light blue hexahedron, which is the minimal processing element (PE) of a real 3D digital image. Then, the way to produce an HSF is building the connections of all the cells in the ACC. More exactly, and in order to promote an efficient parallel computation, we built three trees: the (0, 1), (1, 2) and (2, 3) trees. More details about crack transports and time orders of parallel HSF computation can be consulted in [21].

In the present paper, some restrictions still remain on our HSF software, like considering only 6-adjacency for FG voxels. Whereas this restriction impedes us to present abundant testing with real images in order to capture their homotopy-based features, it is sufficient for distinguishing complex patterns from synthetic images.

According to the generation of a HSF structure, each critical 0-cell of a color has a link (vector of cells) that connects with the opposite color. Thus, the nesting of components (and then the classical Region-Adjacency Tree) can be easily found. Moreover, those critical cells of higher dimensions can be associated with the component of their border cells. In the case of 3D, tunnels add a valuable information when relating each tunnel with a pair of a FG and a BG components. In addition, cavities (represented by critical 2-cells) have a dual relation with critical 0-cells. From now on, these relations are expressed in the Hom-trees of the processed images, using dashed arcs to enclose related cells. Once the 1 and 2 related cells have been identified, Hom-tree can be simply reduced to the edges that connects the 0-cells (black and white little circles in e.g. Fig. 6) plus a weight indicating the number of tunnels that hang from a component.

A simple but clarifying object is first presented: a foreground ring normal to Z axis (see Fig. 5). In this figure, all the HSF trees for this ring are depicted

using different colors. Meanwhile, thickest lines represent critical cells. For the FG ring, they are one 0-cell (representative of the FG component) and one 1-cell (representative of the FG tunnel). Correspondingly, the BG ambiance that surrounds the ring contains one 0-cell (represented by the most upper right 0-cell), one 1-cell (because the FG ring is seen like a tunnel for the BG) and a 2-cell, representative of the cavity (which is indeed the FG ring). Finally, the Hom-tree of the image in Fig. 5 can be summarized in Fig. 6, Left. Note that each connected component of every color is associated with its corresponding critical cells.

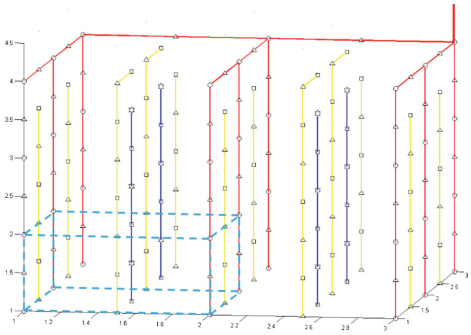

Fig. 4. A visual representation of the scenario where the digital image will be "embedded". 0-cells, 1-cells, 2-cells and 3-cells are represented by circles, triangles, squares and stars respectively. At the left bottom of the figure there is a representation of a voxel as a light blue hexahedron, which is the minimal processing element (PE) of a real 3D digital image. (Color figure online)

More complicated images can be topologically classified with the Hom-tree representation. In Fig. 6, right, we depict the Hom-tree of a binary image containing a FG sphere surrounding a FG torus. From top to bottom for the 0-cells, we distinguish the following: (1) Firstly the 0-cell of the BG canvas that has no dual correspondence; (2) Secondly, the FG sphere representative (which is related to the cavity of previous 0-cell); (3) A new BG 0-cell related to the cavity of the FG sphere; (4) the 0-cell of the torus that is linked with the previous BG component. Between these two previous 0-cells there is interface (a red edge in this Fig. 6) weighted with 1, because the outer tunnel of the torus can be delineated using a line that resides in the sphere cavity. And finally, (5) the last BG component is the cavity of the torus, with hold the delineation of the inner tunnel of the torus (thus the last red edge is also weighted with 1. The fact that each critical cell has its corresponding dual (except the BG component of the canvas) means that the Euler number of the whole 3D image is simply 1.

Finally, Hom-Tree is able to distinguishing non-isotopic patterns. An interesting example occurs for spheres with handles. In Fig. 7 a HSF of a FG sphere with two external handles is completely drawn to distinguish that the borders

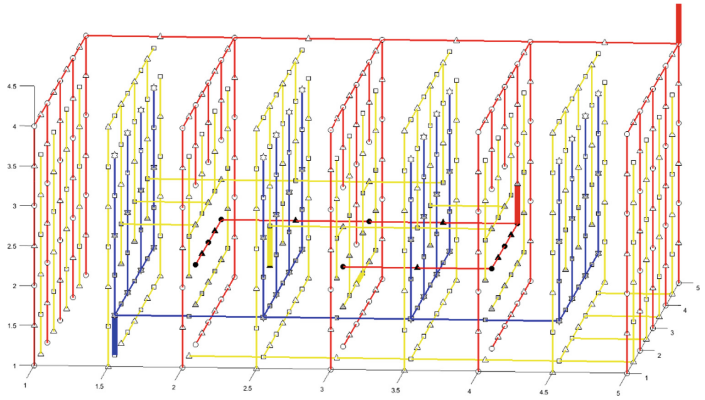

Fig. 5. A foreground ring normal to Z axis is depicted along with the computation of a HSF structure. $(0,1)$-HSF-trees are displayed in red, $(1,2)$-HSF-trees in yellow and $(2,3)$-HSF-trees in blue. The thickest line of every tree represents the critical cell of its corresponding tree. (Color figure online)

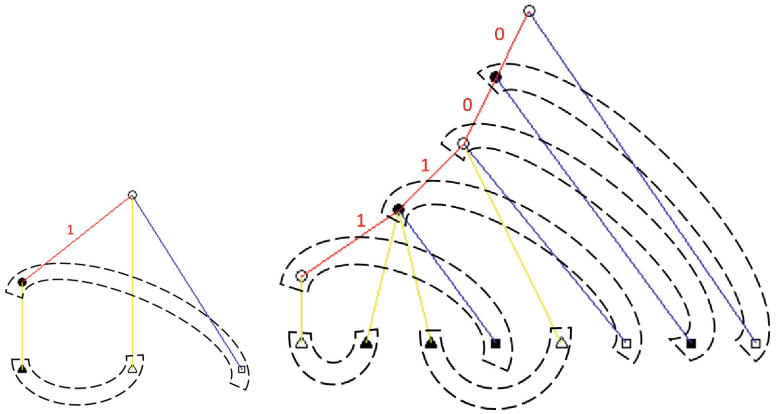

Fig. 6. Left: Hom-tree for the previous foreground ring of Fig. 5. Same color convention is followed. Solid symbols are for foreground cells and hollow symbols for the background ones. An example of the duality of the HSF is showed pairing every critical cell of the FG with its corresponding BG counterpart (excepting the BG critical cell of the canvas, which is the root of the tree). These associations are shown with dashed arcs. In this case, the BG canvas has only one cavity that is associated to the FG component, and the FG tunnel is directly associated with the BG tunnel. Right: Hom-tree for an image containing a FG sphere that in turn surrounds a FG torus. Note that each critical cell has its corresponding dual (except the BG component of the canvas). (Color figure online)

of its two critical 1-cells (marked with thickest yellow lines at $Z = 2$, $Y = 2$, $X = 2.5$ and $X = 6.5$) fall into the FG component. Moreover, there are two additional tunnels for the BG external component (ahead of the two previous ones

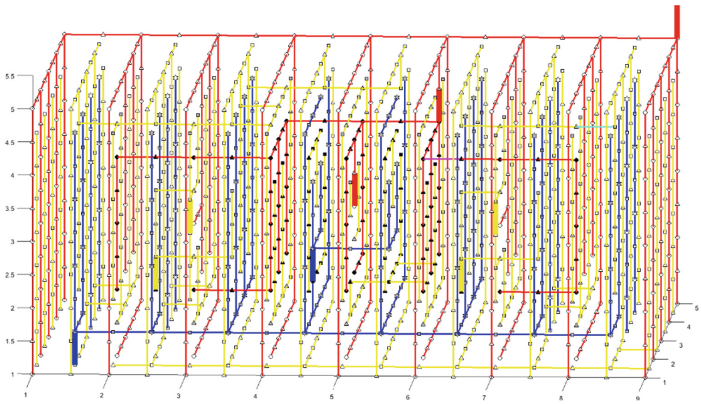

Fig. 7. HSF of a sphere with two external handles. The colors code is the same as the employed for the previous figures. All trees are being displayed along with their corresponding critical cells. In the upper right part of the figure, a red link represents the BG CC of the image. (Color figure online)

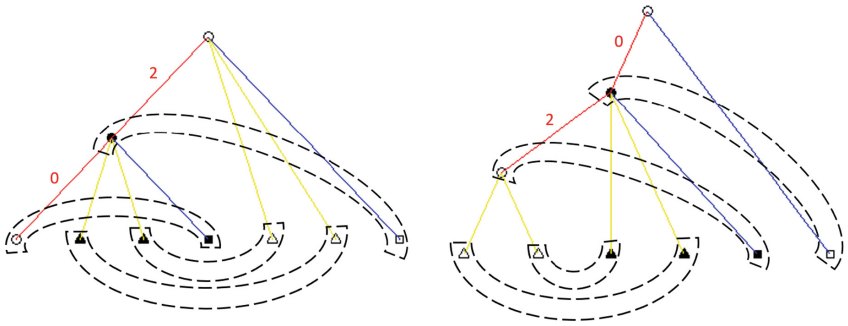

Fig. 8. Left: Hom-tree for the previous foreground sphere with two external handles. Same color convention is followed. Solid symbols are for foreground cells and hollow symbols for the background ones. The root node corresponds to the BG critical 0-cell of the canvas in which the image in embedded. Every critical cell will have a dual nature, i.e. for every FG critical cell can be associated a BG critical cell (these parings are shown with dashed arcs), excepting the critical cell corresponding to the canvas. Right: Hom-Tree for a foreground sphere with two inner handles. Although the FG component has the same Hom-Tree, the most inner BG component contains now the two tunnels that was associated to the BG canvas on the left Hom-Tree. (Color figure online)

at $Y = 1.5$). As a result, its condensed Hom-tree (see Fig. 8, left) is composed by three connected components whose edges from top to bottom have weights 2 and 0. On the other hand, for the sphere with two internal handles, (see Fig. 8, right), its RAG coincides with the previous one, but the tunnels are delineated

here within the sphere cavity. That means that the weights for the Hom-tree edges are now (from top to bottom) 0 and 2.

Nevertheless, it is worth to mention that some dissimilar nesting of digital objects cannot be distinguished using the Hom-tree representation: this is the case of a torus versus a sphere with an inner tunnel and an external one. Both of them result with the same Hom-tree representation and edge weights.

5 Conclusions

We present Hom-tree as an compressed representation of a 3D binary digital image I. It is an edge-weighted RAG Tree of black 6-CCs and white 26-CCs, with weights measured in terms of "common" tunnels of neighbors CCs. An algorithm for computing a Hom-Tree via a HSF model of I is presented and its isotopic invariance is validated with several synthetic images. This concept surpasses the classical RAG Tree with regard to topological classification tasks. Moreover, this representation allows to define graph-based operations for modifying it [25] (e.g. splitting and merging of regions,...) in order to develop a Solid Constructive Topology theory. Also, potential applications of the Hom-Tree structure (possibly, with weights representing geometrical and analytic properties, like area, volume, delineations lengths,...) can be explored for retrieval, classification, recognition and registrations tasks on biomedical digital images.

In a near future, we plan:

(a) To implement a fully parallel algorithm for computing the Hom-Tree from an HSF model.
(b) To extend this notion to grey-level and color images (extending the classical Region-Adjacency-Graph notion) and to higher dimension (3D+t, 4D, nD) and to mimic the Hom-Tree parallel computation via HSF model to these more complex contexts.

In the longer term, we will try to enrich the Hom-Tree structure with more complex topological (mainly, homological) characteristics of the CCs of I, in order to distinguish, for example, a torus from a sphere with an internal and an external handle.

References

1. Ansaldi, S., De Floriani, L., Falcidieno, B.: Geometric modeling of solid objects by using a face adjacency graph representation. In: ACM SIGGRAPH Computer Graphics, vol. 19, no. 3, pp. 131–139. ACM, July 1985
2. Bertrand, G.: Simple points, topological numbers and geodesic neighborhoods in cubic grids. Pattern Recogn. Lett. **15**, 1003–1011 (1994)
3. Cardoze, D.E., Miller, G.L., Phillips, T.: Representing topological structures using cell-chains. In: Kim, M.-S., Shimada, K. (eds.) GMP 2006. LNCS, vol. 4077, pp. 248–266. Springer, Heidelberg (2006). https://doi.org/10.1007/11802914_18

4. Costanza, E., Robinson, J.: A region adjacency tree approach to the detection and design of fiducials. In: Video, Vision and Graphics, pp. 63–99 (2003)
5. Cucchiara, R., Grana, C., Prati, A., Seidenari, S., Pellacani, G.: Building the topological tree by recursive FCM color clustering. In: Object Recognition Supported by User Interaction for Service Robots, vol. 1, pp. 759–762. IEEE, August 2002
6. Cohn, A., Bennett, B., Gooday, J., Gotts, N.: Qualitative spacial representation and reasoning with the region connection calculus. GeoInformatica **1**(3), 275–316 (1997)
7. Delgado-Friedrichs, O., Robins, V., Sheppard, A.: Skeletonization and partitioning of digital images using discrete Morse theory. IEEE Trans. Pattern Anal. Mach. Intell. **37**(3), 654–666 (2015)
8. Díaz-del-Río, F., Real, P., Onchis, D.: Labeling color 2D digital images in theoretical near logarithmic time. In: Felsberg, M., Heyden, A., Krüger, N. (eds.) CAIP 2017. LNCS, vol. 10425, pp. 391–402. Springer, Cham (2017). https://doi.org/10.1007/978-3-319-64698-5_33
9. Díaz-del-Río, F., Real, P., Onchis, D.M.: A parallel homological spanning forest framework for 2D topological image analysis. Pattern Recogn. Lett. **83**, 49–58 (2016)
10. Forman, R.: Morse theory for cell complexes. Adv. Math. **134**, 90–145 (1998)
11. Klette, R., Rosenfeld, A.: Digital Geometry Geometric: Methods for Digital Picture Analysis. Morgan Kaufmann, San Francisco (2004)
12. Klette, G.: Skeletons in digital image processing. CITR, The University of Auckland, New Zealand (2002)
13. Klette, R., Rosenfeld, A.: Digital Geometry: Geometric Methods for Digital Picture Analysis. Elsevier, Amsterdam (2004)
14. Kong, T.Y., Rosenfeld, A.: Topological Algorithms for Digital Image Processing, vol. 19. Elsevier, Amsterdam (1996)
15. Kong, T.Y., Roscoe, A.W.: A theory of binary digital pictures. Comput. Vis. Graph. Image Process. **32**(2), 221–243 (1985)
16. Kovalevsky, V.: Algorithms in digital geometry based on cellular topology. In: Klette, R., Žunić, J. (eds.) IWCIA 2004. LNCS, vol. 3322, pp. 366–393. Springer, Heidelberg (2004). https://doi.org/10.1007/978-3-540-30503-3_27
17. Lienhardt, P.: Topological models for boundary representation: a comparison with n-dimensional generalized maps. Comput. Aided Des. **23**(1), 59–82 (1991)
18. Molina-Abril, H., Real, P., Nakamura, A., Klette, R.: Connectivity calculus of fractal polyhedrons. Pattern Recogn. **48**(4), 1150–1160 (2015)
19. Molina-Abril, H., Real, P.: Homological spanning forest framework for 2D image analysis. Ann. Math. Artif. Intell. **64**(4), 385–409 (2012)
20. Pavlidis, T.: Algorithms for Graphics and Image Processing. Springer, Heidelberg (1997)
21. Real, P., Molina-Abril, H., Díaz-del-Río, F., Blanco-Trejo, S., Onchis, D.: Enhanced parallel generation of tree structures for the recognition of 3D images. In: Carrasco-Ochoa, J., Martínez-Trinidad, J., Olvera-López, J., Salas, J. (eds.) MCPR 2019. LNCS, vol. 11524, pp. 292–301. Springer, Cham (2019). https://doi.org/10.1007/978-3-030-21077-9_27
22. Real, P., Diaz-del-Rio, F., Onchis, D.: Toward parallel computation of dense homotopy skeletons for nD digital objects. In: Brimkov, V.E., Barneva, R.P. (eds.) IWCIA 2017. LNCS, vol. 10256, pp. 142–155. Springer, Cham (2017). https://doi.org/10.1007/978-3-319-59108-7_12

23. Rosenfeld, A.: Adjacency in digital pictures. Inf. Control **26**(1), 24–33 (1974)
24. Serra, J.: Image Analysis and Mathematical Morphology. Academic Press, Cambridge (1982)
25. Stell, J., Worboys, M.: Relations between adjacency trees. Theoret. Comput. Sci. **412**(34), 4452–4468 (2011)